15th World Congress on Computational Mechanics (WCCM-XV)
8th Asian Pacific Congress on Computational Mechanics (APCOM-VIII)
Virtual Congress: 31 July – 5 August 2022
S. Koshizuka (Ed.)

VALIDATION OF DEM USING MACROSCOPIC STRESS-STRAIN BEHAVIOR AND MICROSCOPIC PARTICLE MOTION IN SHEARED GRANULAR ASSEMBLIES

USMAN ALI[1], MAMORU KIKUMOTO[2], MATTEO ORYEM CIANTIA[3] AND YING CUI[4]

[1]Department of Civil Engineering, Yokohama National University
Tokiwadai 79, Hodogaya, Yokohama, Kanagawa 240-8501, Japan
ali-usman-dp@ynu.jp

[2]Department of Civil Engineering, Yokohama National University
Tokiwadai 79, Hodogaya, Yokohama, Kanagawa 240-8501, Japan
kikumoto@ynu.ac.jp

[3]School of Science and Engineering, University of Dundee
Nethergate, Dundee DD1 4HN, Scotland, United Kingdom
m.o.ciantia@dundee.ac.uk

[4]Department of Civil Engineering, Yokohama National University
Tokiwadai 79, Hodogaya, Yokohama, Kanagawa 240-8501, Japan
sai-ei-mx@ynu.ac.jp

Key words: Biaxial shearing, granular material, microscopic mechanism, particle rotation, numerical simulation

Abstract. *Validation and/or calibration of distinct element method (DEM) models is usually performed by comparing element test simulation results with the corresponding stress-strain relationships observed in the laboratory* [1]. *However, such a validation procedure performed at the macroscopic level does not ensure capturing the microscopic particle-level motion* [2]. *Thus, the reliability of the DEM model may be limited to some stress paths and may not hold when the material response becomes non-uniform for example when shear bands develop. In this study, the validity of the DEM is assessed by comparing the numerical result with experimental data considering both particle-scale behavior (including particle rotations) and macroscopic stress-strain characteristics observed in shearing tests on granular media. Biaxial shearing tests were conducted on bi-disperse granular assemblies composed of around 2700 circular particles under different confining pressures. Particle-level motions were detected by a novel image analysis technique. Particle rotations are observed to be a key mechanism for the deformation of granular materials. The results from this study suggest that to properly calibrate DEM models able to capture the mechanical behavior in a more realistic way particle scale motions observed in laboratory experiments along with macroscopic response are necessary.*

1 INTRODUCTION

Prediction of ground deformation and failure is an important issue in the design of soil structures. Ground deformation and failure are often predicted using continuum analysis methods based on constitutive laws for soils [3]. However, geomaterials are discontinuous granular materials composed of solid-phase particles and pore fluids at the microscopic level. The small-scale mechanism that occurs at the particle level is responsible for the large-scale behavior of granular materials [4]. Therefore, to grasp the macroscopic mechanical behavior of granular materials, it is necessary to understand the microscopic mechanical mechanisms that occur between individual particles [5]. The response of geomaterials as granular materials is often modeled by the discrete element method (DEM), which can explicitly model each particle one by one [6]. DEM was introduced by [7] and has become the most common method for simulating the behavior of discrete materials. Unlike the conventional laboratory tests, in DEM the detailed particle-level information can be observed and analyzed which makes DEM a powerful tool to study the micro-deformation mechanisms in granular materials [8].

DEM models require a validation/calibration process, and the reliability of the model significantly depends on the parameters chosen. Usually, validation/calibration of the DEM model is done by matching with the macroscopic stress-strain experimental data [1], [9]. The routine laboratory investigations usually provide an overview of the macroscopic response of granular materials, and the particle-level information is insufficient due to the complexities associated with microscopic measurements. For example, particle rotation has always been recognized as an important microscopic deformation mechanism affecting the large-scale behavior of granular materials. However, it is usually overlooked due to the challenges associated with measuring it in the experiment [10], [11].

In DEM studies, after validating the model by matching it with macroscopic experimental data, the model is usually used to investigate the micro-deformation mechanics in granular media [9]. Though, macroscopically validation ensures reasonable capturing of bulk behavior such as stress-strain response but cannot verify the rationality of particle-scale mechanisms. Furthermore, the reliability of the macroscopically validated DEM models may be limited to some specific stress paths and may not hold reasonably when the testing conditions changed, or deformations become non-uniform such as localized deformations. Some researchers have already realized that the reliability of DEM is significantly dependent on particle-scale parameters [2]. Therefore, a detailed validation/calibration should also consider the particle-scale response of the granular assemblies along with the macroscopic experimental data to enhance the reliability of DEM models.

In this study, a series of biaxial shearing tests are conducted using a bi-disperse mixture of around 2700 circular aluminum rod particles. The kinematics of each particle is identified during shearing by a novel image analysis technique. The particle rotations observed in the experiment are found to be an important particle-scale mechanism significantly influencing the large-scale behavior. We compare our experiment with 2-dimensional DEM. The validation of the DEM model is performed by comparing it with the macroscopic stress-strain response as well as particle-scale rotational behavior observed in the experiment.

2 OUTLINE OF BIAXIAL EXPERIMENT

2.1 Biaxial test apparatus

A schematic view of the biaxial test apparatus is shown in Figure 1. The dimensions of the specimen box are 350 mm x 350 mm at the initial state, and the thickness of the rigid walls is 50 mm. Rigid aluminum walls surround the specimen boundaries, wherein the bottom boundary is fixed, and the top and side boundaries are allowed to move in the normal direction. Load and displacement in both axial and lateral directions are measured. The load is controlled in the lateral direction with a pneumatic cylinder. Meanwhile, either load control with a pneumatic cylinder or displacement control with an electric jack can be arbitrarily switched in the axial direction.

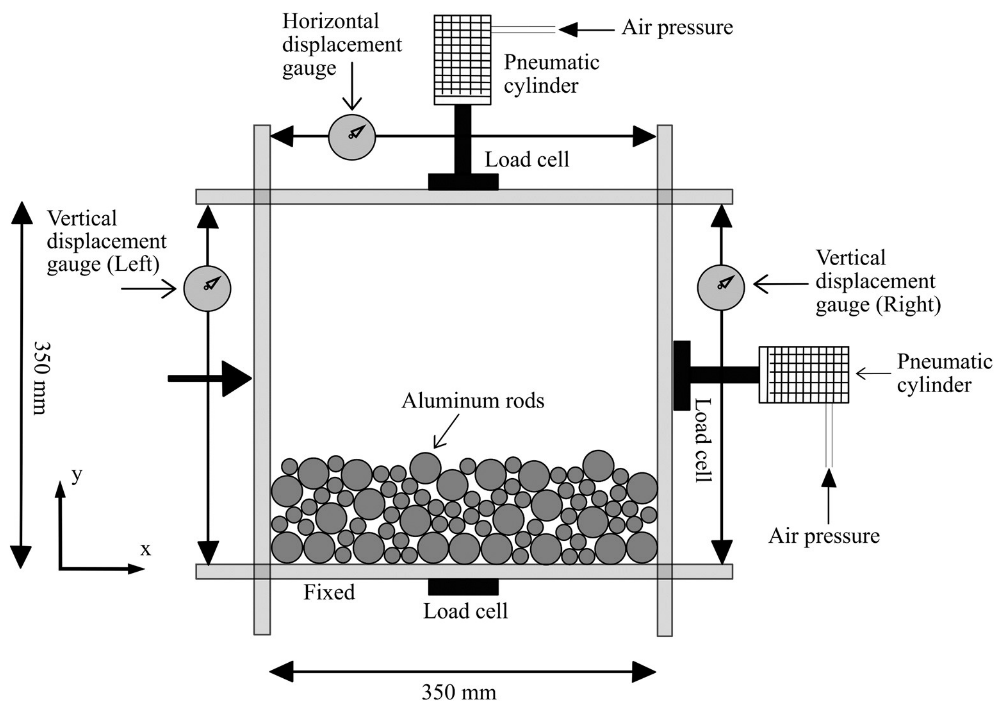

Figure 1: A schematic plan of the biaxial test apparatus

The axial displacement of the top wall is obtained by averaging the displacements of the right and left ends of the wall measured by two displacement transducers. The relative lateral displacement of the side walls is measured by a displacement transducer. Axial and lateral strains are obtained by dividing axial and lateral displacements by the initial height and width of the specimen, respectively. The axial load is obtained by averaging the measurements of two load cells installed at the top and bottom walls, and the lateral load was measured by a load cell installed at the right wall. The displacements and loads in axial and lateral directions are measured by a data logger, and all the data is collected by a computer. The axial and lateral stresses are calculated by dividing the corresponding load by the cross-sectional areas of the specimen perpendicular to each direction, respectively. The cross-sectional areas are continuously updated using the measured lateral and axial displacements. For strain-controlled loading applied in the axial direction, the axial strain rate is controlled by applying a prescribed displacement rate to the cylinder rod with an electric jack. For load-controlled loading in the lateral direction, lateral stresses are continuously monitored by the computer and controlled by sending the target air pressure to the lateral pneumatic cylinder. The air pressure sent to the pneumatic cylinder is maintained by the PC by sending prescribed voltage signals to electro-pneumatic regulators via a digital-analog board.

2.2 Testing material

The granular material used in the experiment comprises dual-size aluminum rods of 10mm and 6mm diameters. The length of all rods is 50 mm, equal to the thickness of the walls of the specimen box. The mixing ratio of big to small particles is 2:3 by weight. Aluminum rod material is widely accepted for studying the mechanical behavior of granular materials under plane strain conditions [12]. The material density of the aluminum rods is 2830 kg/m^3, and the specific weight of the aluminum ground inside the biaxial box is around 22.5 kN/m^3 containing around 2700 particles.

2.3 Image analysis process

The image analysis process includes the preparation of special surface-treated material, image acquisition, particle identification, tracking, and rotation estimation. To increase the accuracy of the image analysis, surface treatment of the material is required before testing to acquire high-quality images during the test. For that, circular black stickers are pasted on the surface of each particle. Each circular sticker contains two dots of red and green color. These dots on the black circular background would help to identify the geometric transformations of particles. During the shearing test, digital images are acquired using a high-quality digital camera. The images are processed to improve the quality by adjusting the intensity and applying other image adjustment techniques using freeware ImageJ. A well-known approach for identifying circular objects in images, MATLAB built-in function ‘imfindcircles’ is used to identify particles. For tracking the particle translations, an algorithm developed by [13] is employed. The trajectories include only the translational movement of the particles, not their rotation. The algorithm developed by [14] named *Multiscale Analysis for Granular Image Correlation* is used to identify particle rotations. The accuracy of rotation algorithms has been evaluated before application. The rotation of stickered particles during the biaxial test can be estimated by a correlation between two consecutive images taken during the test.

3 OUTLINE OF DISCRETE ELEMENT SIMULATION

In recent years, a numerical simulation tool ‘particle flow code’ developed by [15] has emerged as a popular DEM framework and has been applied for investigating granular behavior [16–18]. PFC models simulate the independent movement (translation and rotation) and interaction of many rigid particles that may interact at contacts based on an internal force and moment. Generally, PFC provides a platform for users to develop their codes to resolve various DEM problems. In this regard, the corresponding built-in program FISH is employed to develop the DEM model of the biaxial test. The Hertz contact model based on the theory of Mindlin, and Deresiewicz (1953) is used to describe the interaction between particle-particle and particle-wall. It can produce both normal and shear forces based on the theoretical analysis of the deformation of smooth elastic spheres in frictional contact. This model uses a spring-dashpot response to normal contact between particles and a coulomb friction coefficient for shear interaction. The material parameters used in the numerical simulation are that of the aluminum because in the biaxial experiment aluminum particles are used. All the parameters used are summarized in Table 1.

Table 1: Parameters used in the numerical simulations

Mass density [kg/m^3]	2710
Coefficient of friction, μ particle-particle	0.20
Coefficient of friction, μ particle-wall	0.00
Shear Modulus, G [GPa]	26.0
Poisson's ratio, v	0.30

For numerically simulating the biaxial test, the same scale DEM model is developed i.e., a square specimen box with the same size i.e., 350 mm x 350 mm as used in the experiment. The boundary conditions, particle sizes (10 mm and 6 mm), and mixing ratio (small to big 2:3 by weight) are considered. Figure 2 illustrates the biaxial shear test model of bi-disperse circular disks. σ_1 and σ_3 are principal stresses in the y and x directions, respectively. Samples containing around 2700 particles are generated at almost the same initial void ratio (approximately e = 0.210) as that of the experiment. Simulations are conducted using the same three confining pressures as used in the experiment. Assemblies are first compressed isotropically until the desired confining pressure is achieved and then sheared until the deviatoric strain (ε_s) reaches around 20%.

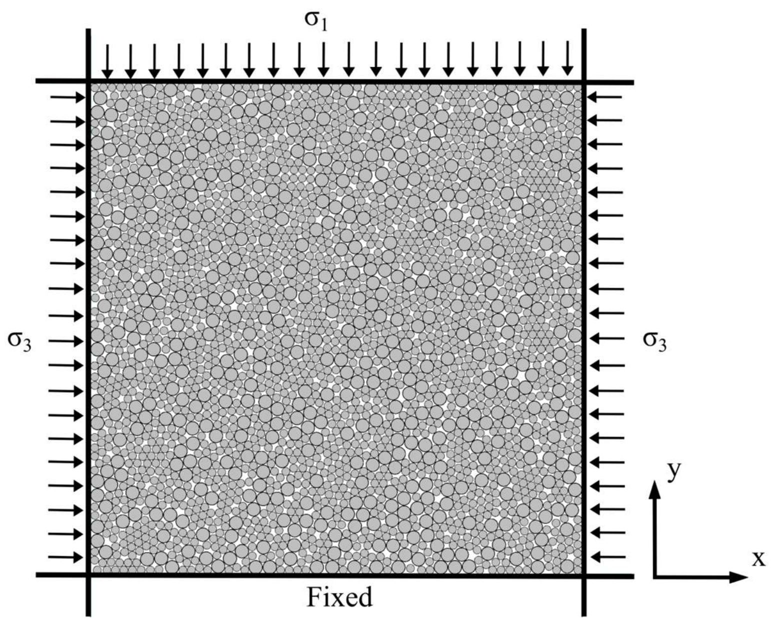

Figure 2: Discrete element model of biaxial shear test

4 VALIDATION OF DISCRETE ELEMENT SIMULATION

4.1 Comparison of macroscopic behavior

The macroscopic stress-strain response and particle rotation results obtained from the experiment are used to validate the DEM model. Figure 3 shows the comparison of the stress-strain relationship and volumetric deformations observed in simulation and experiment using confining pressure of 39.2 kPa. It can be seen that the stress-strain relationships observed in the simulation are very close to the experimental results. The average critical state stress ratio for experiment and simulation is σ_1/σ_3 = 1.83 and 1.77, respectively. The volumetric behavior observed in the simulation is typical and shows a good agreement with the experiment i.e., a slight compression at the start of shearing followed by dilative behavior.

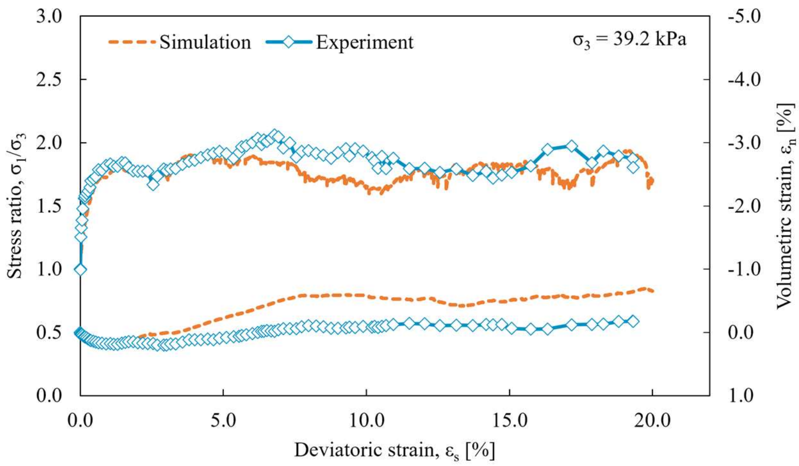

Figure 3: Stress-strain relationship and volumetric behavior of circular aluminum rods observed in experiment and simulation

4.2 Comparison of particle-scale behavior

Figure 4 shows the density histogram of particle rotations, and the dotted line shows the normal fitting for the observed rotations. Particle rotations observed in the simulation show agreement with experimental observation. Generally, in both cases rotations follow a normal distribution around a mean value of approximately 0°. The normal distribution of particle rotations within the granular sample during deformation was also observed by [11, 19]. The number of particles exhibited clockwise rotations is almost equal to the number of particles exhibited counterclockwise rotations. Commonly, in both cases, a clockwise rotating particle is usually accompanied by an opposite rotating particle within the neighboring region. However, in some cases, a group of particles (clusters) exhibits rotation in the same direction accompanied by another opposite rotating cluster in the neighboring region. The formation of rotation clusters within biaxial circular assemblies was also observed by [20].

Figure 5 shows the history of absolute mean rotation for particles for the complete assembly observed in the experiment and simulation. It can be seen that the mean absolute rotation growth in the simulation is fairly close to experimental growth indicating that the DEM model can also reasonably capture the particle-scale rotational behavior. The absolute average rotation observed at the end of shearing for all the particles in the experiment and simulation is 18.6° and 21.2°, respectively. Furthermore, the rotational behavior is observed to be independent of the magnitude of the confining pressure.

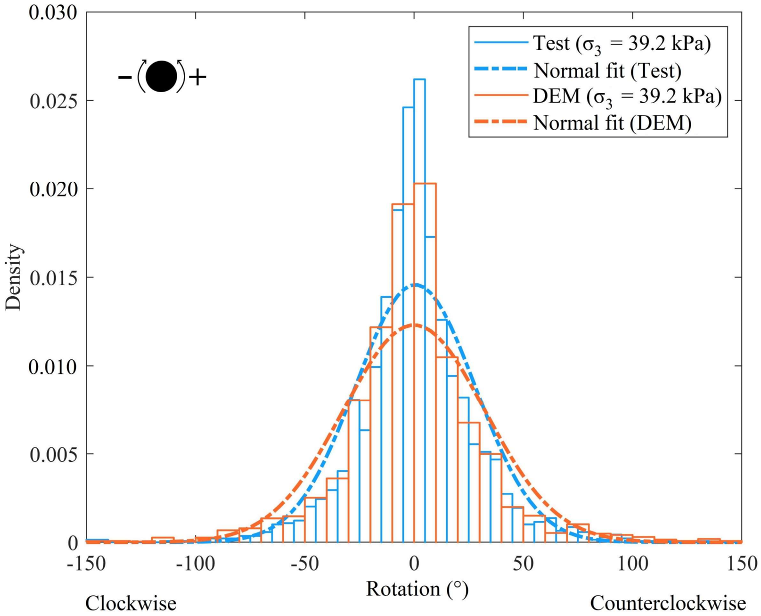

Figure 4: Histograms showing particle rotation density distribution in test and simulation at the end of shearing

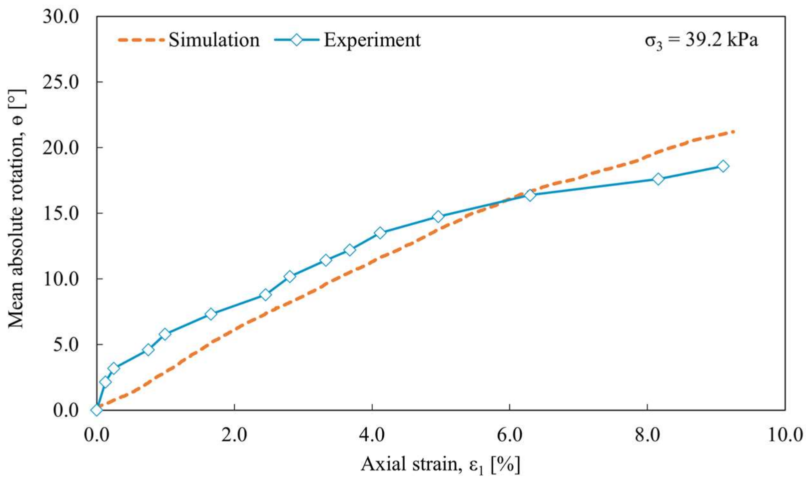

Figure 5: History of mean absolute rotation for complete assembly

Shear band identification: During non-uniform granular deformations such as the formation of a shear band, the particle rotations tend to concentrate inside the shear band i.e., rotation localization [21, 22]. Once the shear band forms, the overall behavior is dominated by it so particle behavior inside the shear band is of significant concern. To identify the particles inside the shear band, a nominal deviatoric strain is assigned to each particle by using a procedure developed for DEM post-processing by [23]. In this procedure, available within YADE, a Voronoi cell hosting each particle is created using a regular Delaunay triangulation having as vertices the mass centers of the labeled grains [24]. Thus, the particle positions at two instants towards the end of shearing (when deviatoric strain is 16% and 20%) were identified and introduced in YADE. Displacements of neighboring grains were then used to compute a nominal displacement gradient tensor for the triangles whose vertices are the centers of each particle. A nominal averaged deviatoric strain was projected back to each grain and a threshold value of strain was used to assign grains to the shear band. The same procedure was applied to identify the particles inside the shear band by [22]. The results of the shear band identification procedure are shown in Figure 6, in which the black grains form the shear band. In both cases, two X-shape shear bands are found to be aligned along the diagonals of the biaxial box. Due to rigid boundary conditions, the lateral displacement is uniform on both sides of the sample and restricts the formation of a typical shear band such as with flexible lateral boundaries. The threshold value of nominal averaged deviatoric strain is set at 0.05 (possible range 0.05-0.2).

Commonly, particles inside the shear band are observed to rotate more. The particles outside the shear band only exhibit significant rotations at the start of the shearing but particles inside the shear bands continue to exhibit rotations even at the end of shearing. Furthermore, in both cases, higher rotations inside the shear bands are found to be associated with low coordination numbers. This confirms that the DEM model could reasonably capture the particle-scale behavior even when the deformation is non-uniform i.e., inside the shear band.

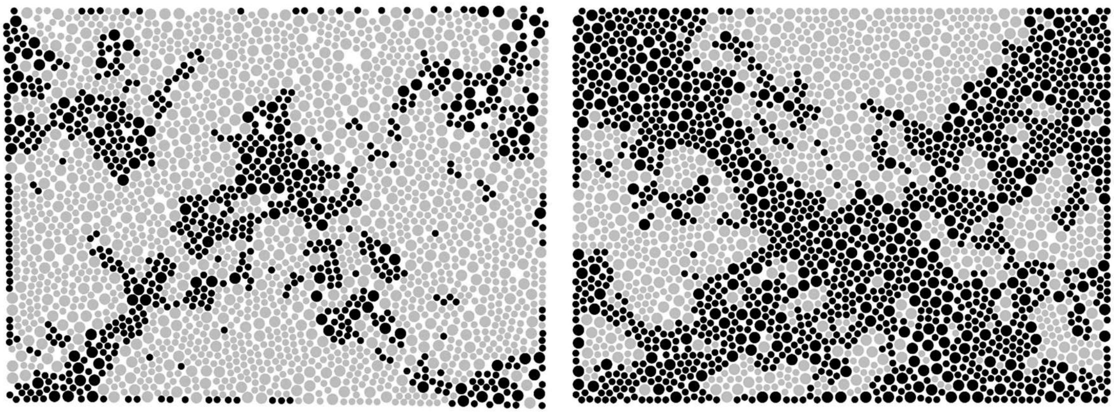

(a) (b)

Figure 6: Shear band identification (a) Experiment (b) Simulation. Particles inside the shear band are colored black.

Effect of particle size on rotational behavior: Figure 7 shows the rotation density distribution histograms observed in the experiment and simulation based on the size of the particles. Dotted lines represent the normal fitting curves. Interestingly, a clear difference in magnitude of rotation is observed between the small and big particles in both cases. Commonly, big particles histograms show higher concentration around the mean i.e., 0° indicating that big particles are relatively resistant to rotation. The mean absolute rotation ratio observed for the small to big particles in the experiment and simulation is 1.7 and 1.8, respectively which indicates that small particles nearly rotate twice as compared to big particles in both cases. This difference of rotation will induce a ball bearing type effect in which the small particles act like a ball bearing between the big particles and may contribute to the strength reduction. A similar effect of small particles in binary mixtures was also observed by [25, 26].

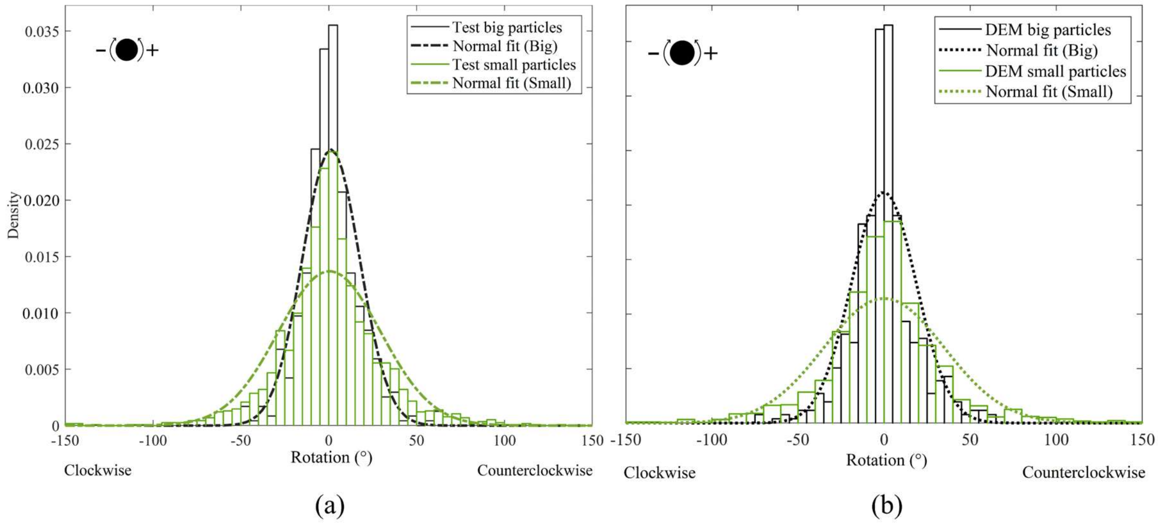

Figure 7: Histograms showing size-wise particle rotation density distribution at the end of shearing (σ_3=39.2kPa) a) Experiment b) Simulation

5 CONCLUSIONS

In this study, a series of biaxial shearing tests are conducted in the laboratory and simulated numerically using DEM. The particle kinematics were detected in the experiment by a novel image analysis technique. Particle rotations are observed to be a key particle scale mechanism. The validation of the DEM model is performed by comparing numerical results with experimental data including macroscopic stress-strain response and particle-scale behavior. Based on the comparison between experimental and numerical data, the conclusions reached are the following:

1) The DEM simulation with the Hertz-Mindlin contact model can successfully capture the experimental macroscopic stress-strain as well as particle-scale response (particle rotation) of granular material in the biaxial shearing mode.
2) Furthermore, the model can also reasonably grasp the similar localized deformation zones and particle-level behavior inside these zones.
3) The ball-bearing effect induced by higher rotation of small particles is also well captured in the simulation. In bi-disperse assemblies used in this study, on average a smaller particle rotates almost twice a big particle.
4) Finally, the validation process of the DEM model to predict the realistic granular behavior requires comparing numerical results with experimental data at macroscopic as well as particle-scale levels to improve the efficiency and reliability of DEM.

ACKNOWLEDGEMENT

Ministry of Education, Culture, Sports, Science, and Technology of Japan is acknowledged for giving financial assistance through the Monbukagakusho scholarship to the first author to study at Yokohama National University, Japan. We also gratefully acknowledge the financial support provided by the Royal Society International Exchanges research grant (IES/R1/201238).

REFERENCES

[1] Z. Y. Huang, Z. X. Yang, and Z. Y. Wang, "Discrete element modeling of sand behavior in a biaxial shear test," *J. Zhejiang Univ. Sci. A*, vol. 9, no. 9, pp. 1176–1183, 2008, doi: 10.1631/jzus.A0720059.

[2] Z. X. Tong, L. W. Zhang, and M. Zhou, "DEM simulation of biaxial compression experiments of inherently anisotropic granular materials and the boundary effects," *J. Appl. Math.*, vol. 2013, 2013, doi: 10.1155/2013/394372.

[3] M. Jiang, H. Zhu, and X. Li, "Strain localization analyses of idealized sands in biaxial tests by distinct element method," *Front. Archit. Civ. Eng. China*, vol. 4, no. 2, pp. 208–222, 2010, doi: 10.1007/s11709-010-0025-2.

[4] E. Andò, S. A. Hall, G. Viggiani, J. Desrues, and P. Bésuelle, "Grain-scale experimental investigation of localised deformation in sand: A discrete particle tracking approach," *Acta Geotech.*, vol. 7, no. 1, pp. 1–13, 2012, doi: 10.1007/s11440-011-0151-6.

[5] S. H. Liu, Y. P. Yao, Q. C. Sun, T. J. Li, and M. Z. Liu, "Microscopic study on stress-strain relation of granular materials," *Chinese Sci. Bull.*, vol. 54, no. 23, pp. 4349–4357, 2009, doi: 10.1007/s11434-009-0599-z.

[6] K. Wu, S. Liu, W. Sun, and S. Rémond, "DEM study of the shear behavior and formation of shear band in biaxial test," *Adv. Powder Technol.*, vol. 31, no. 4, pp. 1431–1440, 2020, doi: 10.1016/j.apt.2020.01.016.

[7] P. A. Cundall, "A discrete numerical model for granular assemblies," *Geeotechnique*, vol. 29, no. 29. pp. 47–65, 1979, [Online]. Available: https://www.icevirtuallibrary.com/doi/abs/10.1680/geot.1979.29.1.47.

[8] S. Yimsiri and K. Soga, "Dem analysis of soil fabric effects on behaviour of sand," *Geotechnique*, vol. 60, no. 6, pp. 483–495, 2010, doi: 10.1680/geot.2010.60.6.483.

[9] M. Nitka and A. Grabowski, "Shear band evolution phenomena in direct shear test modelled with DEM," *Powder Technol.*, vol. 391, pp. 369–384, 2021, doi: 10.1016/j.powtec.2021.06.025.

[10] J. P. Bardet, "Observations on the effects of particle rotations on the failure of idealized granular materials," *Mech. Mater.*, vol. 18, no. 2, pp. 159–182, 1994, doi: 10.1016/0167-6636(94)00006-9.

[11] A. Misra and H. Jiang, "Measured Kinematic Fields in the Biaxial Shear of Granular Materials," *Comput. Geotech.*, vol. 20, no. 3–4, pp. 267–285, 1997, doi: 10.1016/s0266-352x(97)00006-2.

[12] M. Schneebeli, "Mechanique des soils-Une analogie mechanique pour les terres sans cohesion," *Comptes Rendes Hebdomaires des Seances l'Academie des Sci.*, vol. 243, pp. 125–126, 1956, Accessed: May 28, 2021. [Online]. Available: http://ci.nii.ac.jp/naid/10006385613/en/.

[13] J. C. Crocker and D. G. Grier, "Methods of digital video microscopy for colloidal

studies," *J. Colloid Interface Sci.*, vol. 179, no. 1, pp. 298–310, 1996, doi: 10.1006/jcis.1996.0217.

[14] Z. Chen, M. Omidvar, K. Li, and M. Iskander, "Particle rotation of granular materials in plane strain," *Int. J. Phys. Model. Geotech.*, vol. 17, no. 1, pp. 23–40, 2017, doi: 10.1680/jphmg.15.00046.

[15] Itasca Consulting Group Inc., "PFC2D 7.0 Documentation."

[16] M. O. Ciantia, M. Arroyo, C. O'Sullivan, and A. Gens, "Micromechanical inspection of incremental behaviour of crushable soils," *Acta Geotech.*, vol. 14, no. 5, pp. 1337–1356, 2019, doi: 10.1007/s11440-019-00802-0.

[17] Z. Nie, C. Fang, J. Gong, and Z. Liang, "DEM study on the effect of roundness on the shear behaviour of granular materials," *Comput. Geotech.*, vol. 121, no. September 2019, p. 103457, 2020, doi: 10.1016/j.compgeo.2020.103457.

[18] M. Wu, L. Xiong, and J. Wang, "DEM study on effect of particle roundness on biaxial shearing of sand," *Undergr. Sp.*, vol. 6, no. 6, pp. 678–694, 2021, doi: 10.1016/j.undsp.2021.03.006.

[19] M. Oda, J. Konishi, and S. Nemat-Nasser, "Experimental Micromechanical Evaluation of Strength of Granular Materials: Effects of Particle Rolling," *Mech. Mater.*, no. 1, pp. 269–283, 1982.

[20] M. R. Kuhn and K. Bagi, "Particle rotations in granular materials," *15th ASCE Eng. Mech. Conf.*, vol. 6, no. June 2002, 2002.

[21] K. Iwashita and M. Oda, "Rolling Resistance At Contacts in Simulation of Shear Band," *J. Eng. Mech.*, vol. 124, no. March, pp. 285–292, 1998.

[22] R. Rorato, M. Arroyo Alvarez de Toledo, E. C. G. Andò, A. Gens, and G. Viggiani, "Linking shape and rotation of grains during triaxial compression of sand," *Granul. Matter*, vol. 22, no. 4, pp. 1–21, 2020, doi: 10.1007/s10035-020-01058-2.

[23] E. Catalano, B. Chareyre, and E. Barthélémy, "Pore-scale modeling of fluid-particles interaction and emerging poromechanical effects," *Int. J. Numer. Anal. Methods Geomech.*, vol. 38, no. 1, pp. 51–71, Jan. 2014, doi: 10.1002/nag.2198.

[24] V. Šmilauer, E. Catalano, B. Chareyre, S. Dorofeenko, and C. Jakob, "Yade Documentation." p. 526, 2015, doi: https ://doi.org/10.5281/zenod o.34073.

[25] L. E. Vallejo, "Interpretation of the limits in shear strength in binary granular mixtures," *Can. Geotech. J.*, vol. 38, no. 5, pp. 1097–1104, 2001, doi: 10.1139/cgj-38-5-1097.

[26] T. UEDA, T. MATSUSHIMA, and Y. YAMADA, "Ball-Bearing Effect on Shear Behavior of Binary Granular Mixture," *J. Japan Soc. Civ. Eng. Ser. A2 (Applied Mech.*, vol. 68, no. 1, pp. 1–9, 2012, doi: 10.2208/jscejam.68.1.